

J-GEM observations of an electromagnetic counterpart to the neutron star merger GW170817

Yousuke UTSUMI¹, Masaomi TANAKA², Nozomu TOMINAGA^{3,4}, Michitoshi YOSHIDA⁵, Sudhanshu BARWAY⁶, Takahiro NAGAYAMA⁷, Tetsuya ZENKO⁸, Kentaro AOKI⁵, Takuya FUJIYOSHI⁵, Hisanori FURUSAWA², Koji S. KAWABATA¹, Shintaro KOSHIDA⁵, Chien-Hsiu LEE⁵, Tomoki MOROKUMA⁹, Kentaro MOTOHARA⁹, Fumiaki NAKATA⁵, Ryou OHSAWA⁹, Kouji OHTA⁸, Hirofumi OKITA⁵, Akito TAJITSU⁵, Ichi TANAKA⁵, Tsuyoshi TERAJ⁵, Naoki YASUDA⁴, Fumio ABE¹⁰, Yuichiro ASAKURA^{10,†}, Ian A. BOND¹¹, Shota MIYAZAKI¹², Takahiro SUMI¹², Paul J. TRISTRAM¹³, Satoshi HONDA¹⁴, Ryosuke ITOH¹⁵, Yoichi ITOH¹⁴, Miho KAWABATA¹⁶, Kumiko MORIHANA¹⁷, Hiroki NAGASHIMA¹⁶, Tatsuya NAKAOKA¹⁶, Tomohito OHSHIMA¹⁴, Jun TAKAHASHI¹⁴, Masaki TAKAYAMA¹⁴, Wako AOKI², Stefan BAAR¹⁴, Mamoru DOI⁹, Francois FINET⁵, Nobuyuki KANDA¹⁸, Nobuyuki KAWAI¹⁵, Ji Hoon KIM⁵, Daisuke KURODA¹⁹, Wei LIU^{1,20}, Kazuya MATSUBAYASHI¹⁹, Katsuhiko L. MURATA¹⁵, Hiroshi NAGAI², Tomoki SAITO¹⁴, Yoshihiko SAITO¹⁵, Shigeyuki SAKO^{9,21}, Yuichiro SEKIGUCHI²², Yoichi TAMURA¹⁷, Masayuki TANAKA², Makoto UEMURA¹, Masaki S. YAMAGUCHI⁹ and the J-GEM collaboration

¹Hiroshima Astrophysical Science Center, Hiroshima University, 1-3-1 Kagamiyama, Higashi-Hiroshima, Hiroshima, 739-8526, Japan

²National Astronomical Observatory of Japan, 2-21-1 Osawa, Mitaka, Tokyo 181-8588, Japan

³Department of Physics, Faculty of Science and Engineering, Konan University, 8-9-1 Okamoto, Kobe, Hyogo 658-8501, Japan

⁴Kavli Institute for the Physics and Mathematics of the Universe (WPI), The University of Tokyo Institutes for Advanced Study, The University of Tokyo, 5-1-5 Kashiwa, Chiba 277-8583, Japan

⁵Subaru Telescope, National Astronomical Observatory of Japan, 650 North A'ohoku Place, Hilo, HI 96720, USA

⁶South African Astronomical Observatory, PO Box 9, 7935 Observatory, Cape Town, South Africa

⁷Graduate School of Science and Engineering, Kagoshima University, 1-21-35, Korimoto, Kagoshima, 890-0065, Japan

⁸Department of Astronomy, Kyoto University, Kitashirakawa-Oiwake-cho, Sakyo-ku, Kyoto, 606-8502, Japan

⁹Institute of Astronomy, Graduate School of Science, The University of Tokyo, 2-21-1 Osawa, Mitaka, Tokyo 181-0015, Japan

¹⁰Institute for Space-Earth Environmental Research, Nagoya University, Furo-cho, Chikusa, Nagoya, Aichi 464-8601, Japan

¹¹Institute for Natural and Mathematical Sciences, Massey University, Private Bag 102904

North Shore Mail Centre, Auckland 0745, New Zealand

¹²Department of Earth and Space Science, Graduate School of Science, Osaka University,
1-1 Machikaneyama, Toyonake, Osaka 560-0043, Japan

¹³University of Canterbury, Mt John Observatory, PO Box 56, Lake Tekapo 7945, New Zealand

¹⁴Nishi-Harima Astronomical Observatory, Center for Astronomy, University of Hyogo, 407-2,
Nishigaichi, Sayo, Hyogo 679-5313, Japan

¹⁵Department of Physics, Tokyo Institute of Technology, 2-12-1 Ookayama, Meguro-ku, Tokyo
152-8551, Japan

¹⁶Department of Physical Science, Hiroshima University, Kagamiyama, Higashi-Hiroshima
739-8526, Japan

¹⁷Division of Particle and Astrophysical Science, Graduate School of Science, Nagoya
University, Furo-cho, Chikusa-ku, Nagoya, 464-8602, Japan

¹⁸Department of Physics, Graduate School of Science, Osaka City University, Osaka
558-8585, Japan

¹⁹Okayama Astrophysical Observatory, National Astronomical Observatory of Japan, 3037-5
Honjo, Kamogata, Asakuchi, Okayama 719-0232, Japan

²⁰University of Chinese Academy of Sciences, No.2 Beijing West Road, Purple Mountain
Observatory, Nanjing, 210008, China

²¹Precursory Research for Embryonic Science and Technology, Japan Science and
Technology Agency, 2-21-1 Osawa, Mitaka, Tokyo 181-0015, Japan

²²Department of Physics, Toho University, Funabashi, Chiba 274-8510, Japan

[†]Deceased 18 August 2017

Received 0 0; Accepted 0 0

Abstract

The first detected gravitational wave from a neutron star merger was GW170817. In this study, we present J-GEM follow-up observations of SSS17a, an electromagnetic counterpart of GW170817. SSS17a shows a 2.5-mag decline in the z -band from 1.7 days to 7.7 days after the merger. Such a rapid decline is not comparable with supernovae light curves at any epoch. The color of SSS17a also evolves rapidly and becomes redder for later epochs; the $z - H$ color changed by approximately 2.5 mag in the period of 0.7 days to 7.7 days. The rapid evolution of both the optical brightness and the color are consistent with the expected properties of a kilonova that is powered by the radioactive decay of newly synthesized r -process nuclei. Kilonova models with Lanthanide elements can reproduce the aforementioned observed properties well, which suggests that r -process nucleosynthesis beyond the second peak takes place in SSS17a. However, the absolute magnitude of SSS17a is brighter than the expected brightness of the kilonova models with the ejecta mass of $0.01 M_{\odot}$, which suggests a more intense mass ejection ($\sim 0.03 M_{\odot}$) or possibly an additional energy source.

Key words: Gravitational waves — Stars: neutron — nuclear reactions, nucleosynthesis, abundances

1 Introduction

After the first detections of gravitational wave (GW) events from binary black hole (BBH) coalescence (Abbott et al. 2016a, 2016b, 2017), the detection of GWs from a compact binary coalescence including at least one neutron star (NS) has been eagerly awaited. This is because the compact binary coalescence including an NS is ex-

pected to be accompanied by a variety of electromagnetic (EM) emissions. An optical and near-infrared (NIR) emission driven by the radioactive decays of r -process nuclei, “kilonova” or “macronova” (Li & Paczyński 1998; Kulkarni 2005; Metzger et al. 2010), is one of the most promising EM counterparts. Optical and NIR observations of these events enable us to understand the origin

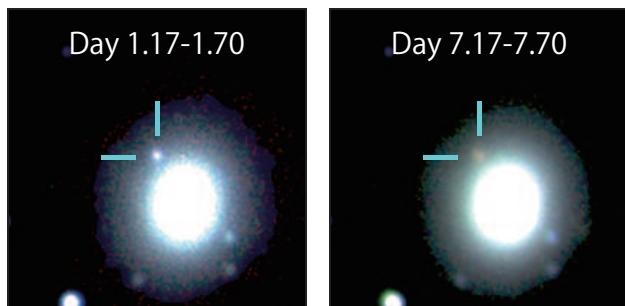


Fig. 1. Three-color composite images of SSS17a using z -, H -, and K_s -band images. The size of the image is 56×56 arcsec². From left to right, the combined images created from the images taken between $t = 1.17$ and 1.70 days and between $t = 7.17$ and 7.70 days are shown.

of r -process elements in the Universe as emission properties reflect the ejected mass and abundances of r -process elements (e.g. Kasen et al. 2013; Barnes & Kasen 2013; Tanaka & Hotokezaka 2013; Tanaka et al. 2014; Metzger & Fernández 2014; Kasen et al. 2015).

On August 17, 2017, 12:41:04 GMT, the LIGO (Laser Interferometer Gravitational-Wave Observatory) Hanford observatory (LHO) identified a GW candidate in an NS merger (The LIGO Scientific Collaboration and the Virgo Collaboration 2017a). The subsequent analysis with three available GW interferometers including the LIGO Livingston Observatory (LLO) and Virgo shrank the localization to 33.6 deg^2 for a 90% credible region (The LIGO Scientific Collaboration and the Virgo Collaboration 2017b) and confirmed the detection (GW170817; The LIGO Scientific Collaboration and the Virgo Collaboration in prep.). A Fermi-GBM trigger, approximately 2 s after the coalescence, coincided with this GW event and provided additional initial information regarding the localization with an error radius of 17.45 deg (The LIGO Scientific Collaboration and the Virgo Collaboration 2017c), which covers the area localized by the GW detectors. Coulter et al. (2017, in prep.) reported a possible optical counterpart SSS17a, within the localization area, near NGC 4993. The source located at $(\alpha, \delta) = (13:09:48.07, -23:22:53.3)$, 10 arcsec away from NGC 4993 (Figure 1), is an S0 galaxy at a distance of $\sim 40 \text{ Mpc}$ (Freedman et al. 2001).

We conducted coordinated observations in the framework of Japanese collaboration for Gravitational-wave Electro-Magnetic follow-up (J-GEM) (Morokuma et al. 2016; Yoshida et al. 2017; Utsumi et al. in press) immediately after the discovery of the strong candidate SSS17a and investigated the characteristics of the optical and NIR emission. In this paper, we present the results of the J-GEM follow-up observations of SSS17a. All magnitudes are given using the unit of AB.

2 J-GEM Observations

A broad geometrical distribution of observatories was required to observe SSS17a because it was visible for a limited amount of time after sunset in the northern hemisphere. J-GEM facilities were suitable for observing this target because they are distributed all over the Earth in terms of the longitude, which included the southern hemisphere where the visibility was better. We used the following facilities to perform follow-up optical observations of GW170817: 8.2 m Subaru / HSC (Miyazaki et al. 2012) and MOIRCS (Suzuki et al. 2008) at Mauna Kea in the United States; 2.0 m Nayuta / NIC (near-infrared imager) at the Nishi-Harima Astronomical Observatory in Japan; 1.8 m MOA-II / MOA-cam3 (Sako et al. 2008; Sumi et al. 2016) and the 61 cm Boller & Chivens telescope (B&C) / Tripol5 at the Mt. John Observatory in New Zealand; 1.5 m Kanata / HONIR (Akitaya et al. 2014) at the Higashi-Hiroshima Astronomical Observatory in Japan; 1.4 m IRSF / SIRIUS (Nagayama et al. 2003) at the South African Astronomical Observatory; and 50 cm MITSuME (Kotani et al. 2005) at the Akeno Observatory in Japan.

We reduced all the raw images obtained using the aforementioned instruments in a standard manner. After eliminating the instrumental signatures, we made astrometric and photometric calibrations. The astrometric calibrations were performed with *astrometry.net* (Lang et al. 2010) using the default reference catalog USNO-B1.0 (Monet et al. 2003), while the PanSTARRS catalog (Chambers et al. 2016) was used for the HSC calibration because it is a standard catalog for the HSC reduction. The number density of stars in the B&C / Tripol5 images was not sufficient for solving the astrometric solution using *astrometry.net*. We therefore used *Scamp* (Bertin 2006) for the B&C / Tripol5 image astrometric calibration instead. The photometric calibrations were performed using the PanSTARRS catalog for the optical data and the 2MASS catalog (Cutri et al. 2003) for the NIR data. We did not apply system transformation for adjusting small differences between the band systems because it required the assumption of a spectrum of the source, except in the case of the MOA-cam3 photometry. The R -band used by MOA-cam3 of MOA-II is largely different from the standard Johnson system. We determined an empirical relation for the differences between the catalog magnitudes and the instrumental magnitudes as a function of the color constructed from the instrumental magnitudes (e.g. Koshimoto et al. 2017). Using Lupton's equation, the catalog magnitudes were converted from the PanSTARRS magnitude to the Johnson system¹. We converted Vega

¹ <http://www.sdss3.org/dr8/algorithms/sdssUBVRITransform.php#Lupton2005>

magnitudes to AB magnitudes using the method specified in Blanton & Roweis (2007).

A large contamination from NGC 4993 was a problem in performing accurate measurement of the flux of SSS17a (Figure 1). In order to minimize the systematic uncertainties in the techniques of background subtraction and photometry used for obtaining our measurements, we applied the same procedure for all the data, which is described as follows. First, we subtracted the host galaxy component from the reduced image using *GALFIT* (Peng et al. 2002). The model employed was a Sersic profile with free parameters describing the position, integrated magnitude, effective radius, Sersic index, axis ratio, and position angle. A PSF model constructed using *PSFEX* (Bertin 2011) was used in the fitting procedure. Once the fitting converged, *GALFIT* generated residual images. We obtained photometry from the images in which the target was clearly visible after the subtraction. We then ran *SExtractor 2.19.5* (Bertin & Arnouts 1996) on the residual images, thus enabling the local sky subtraction with a grid size of 16 pixels—which was larger than the seeing size for all measurements—and the PSF model fitting for photometry. The residuals of the host galaxy subtraction could be reduced owing to this local sky subtraction. We adopted *MAG_POINTSOURCE*, an integrated magnitude of the fitted PSF, as a measure of magnitude and *MAGERR_POINTSOURCE* as the error of the measurements. We confirmed that the measurements for *z*-band obtained from *SExtractor* were consistent with those of *hscPipe*, which is a standard pipeline of HSC reduction (Bosch et al. 2017). We also confirmed that the brightness of a reference star was constant in all the measurements for an individual instrument. The measurements are presented in table 1.

3 Results

The top panel of Figure 2 shows the light curves of SSS17a in various bands based on our photometry. The magnitudes have been corrected for the Galactic extinction by assuming $E(B - V) = 0.10$ mag (Schlafly & Finkbeiner 2011). We do not consider the measurements obtained using Kanata / HONIR, Nayuta / NIC, and MITSuME because the measurements are not reliable owing to the strong contamination from twilight or bad weather.

A remarkable feature of SSS17a is the rapid decline in the *z*-band brightness by 2.5 mag in 6 days. In contrast, the fluxes in the NIR bands decline more slowly than those in the optical band. The densely sampled observations by IRSF / SIRIUS exhibit a slight brightening at the earliest epochs in the *H*- and *K_s*-bands and demon-

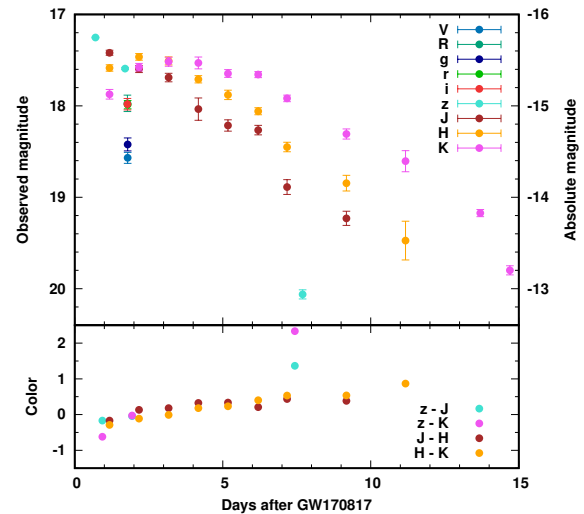


Fig. 2. Light curves and color evolution of SSS17a. The face color is changed with the respective bands. The galactic extinction has been corrected by assuming $E(B - V) = 0.1$ mag (Schlafly & Finkbeiner 2011).

strate that the light curves in the redder bands start to decline subsequently and fade more slowly. The declines in 6 days after the peak are 1.47 mag, 1.33 mag, and 0.96 mag in the *J*-band, *H*-band, and *K_s*-band respectively.

These features are also depicted in the evolution of colors in the *z*-, *J*-, *H*-, and *K_s*-bands (as shown in the bottom panel of Figure 2). The colors in the *z*-band and NIR band rapidly become redder, and the reddening in 6 days are 2.43 mag and 1.00 mag in the $z - K_s$ color and $z - J$ color respectively. In contrast, the reddening in the colors in the NIR bands are as slow as 0.34 mag in the $J - H$ color and 0.83 mag in the $H - K_s$ color. As a result, the optical-NIR color of SSS17a progressively becomes redder with time (Figure 1).

4 Origin of SSS17a

Figure 3 shows the *z*-band light curves for SSS17a, Type Ia supernova (SN Ia, Nugent et al. 2002), Type II plateau supernova (SN IIP, Sanders et al. 2015), and three kilonova models with an ejecta mass of $M_{ej} = 0.01M_{\odot}$ as mentioned by Tanaka et al. (2017). The kilonova models are a Lanthanide-rich dynamical ejecta model and post-merger wind models with a medium Y_e of 0.25 and high Y_e of 0.30. The model with $Y_e = 0.25$ contains a small fraction of Lanthanide elements while that with $Y_e = 0.30$ is Lanthanide-free. The rapid decline of SSS17a is not similar to the properties of known supernovae, and the *z*-band magnitude of SSS17a at $t = 7.7$ days is > 3 mag fainter than supernovae Ia and IIP. However, the rapid decline of SSS17a is consistent with the expected properties of kilo-

Table 1. J-GEM measurements of SSS17a.

Epoch Days	Filter	Mag [†] [AB]	MagErr [AB]	Instrument
0.70	z	17.40	0.01	Subaru / HSC
1.17	J	17.51	0.03	IRSF / SIRIUS
1.17	H	17.64	0.04	IRSF / SIRIUS
1.17	K _s	17.91	0.05	IRSF / SIRIUS
1.70	z	17.74	0.01	Subaru / HSC
1.78	g	18.80	0.07	B&C / Tripol5
1.78	r	18.26	0.04	B&C / Tripol5
1.78	i	18.19	0.06	B&C / Tripol5
1.78	R	18.32*	0.07	MOA-II / MOA-cam3
1.79	V	18.89*	0.07	MOA-II / MOA-cam3
2.17	J	17.69	0.04	IRSF / SIRIUS
2.17	H	17.52	0.04	IRSF / SIRIUS
2.17	K _s	17.61	0.04	IRSF / SIRIUS
3.17	J	17.78	0.05	IRSF / SIRIUS
3.17	H	17.57	0.04	IRSF / SIRIUS
3.17	K _s	17.55	0.05	IRSF / SIRIUS
4.18	J	18.13	0.12	IRSF / SIRIUS
4.18	H	17.77	0.04	IRSF / SIRIUS
4.18	K _s	17.57	0.07	IRSF / SIRIUS
5.18	J	18.31	0.06	IRSF / SIRIUS
5.18	H	17.94	0.05	IRSF / SIRIUS
5.18	K _s	17.68	0.04	IRSF / SIRIUS
6.20	J	18.36	0.05	IRSF / SIRIUS
6.20	H	18.12	0.04	IRSF / SIRIUS
6.20	K _s	17.69	0.03	IRSF / SIRIUS
7.17	J	18.98	0.08	IRSF / SIRIUS
7.17	H	18.51	0.05	IRSF / SIRIUS
7.17	K _s	17.95	0.04	IRSF / SIRIUS
7.70	z	20.21	0.04	Subaru / HSC
9.18	J	19.32	0.08	IRSF / SIRIUS
9.18	H	18.90	0.09	IRSF / SIRIUS
9.18	K _s	18.34	0.06	IRSF / SIRIUS
11.17	H	19.53	0.21	IRSF / SIRIUS
11.17	K _s	18.64	0.12	IRSF / SIRIUS
14.27	K _s	19.35	0.04	Subaru / MOIRCS
15.27	K _s	19.97	0.05	Subaru / MOIRCS

* MOA-II / MOA-cam3 measurements are calibrated using the empirical relation. Uncertainties regarding the conversion are large but not taken into account in the error. † The magnitudes listed here are the values before the Galactic extinction correction.

novae, although SSS17a is 1–3 mag brighter than all the three kilonova models.

The rapid evolution of SSS17a is characterized by a magnitude difference in the z-band (Δz) between $t = 1.7$ days and 7.7 days (6 days interval). The red point in Figure 4 shows the Δz and $i - z$ color at $t = 1.7$ days (see Utsumi et al. in press). For the purpose of comparison, we show Δz in a 6-day interval and $(i - z)_{1st}$ color at the

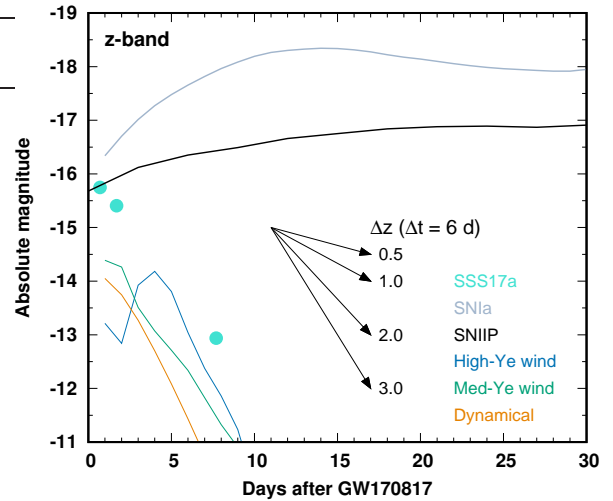


Fig. 3. Absolute magnitude of z-band observations (dots) compared with models of supernovae (in gray curves) and kilonovae (colored curves). The kilonova models are calculated assuming that the mass of the ejecta from a neutron star merger M_{ej} is $0.01M_{\odot}$. The absolute magnitudes of the kilonova models quickly decline as compared with supernovae. The z-band light curve of SSS17a follows the decline of the kilonova models although the observed magnitudes are 1–3 magnitude brighter than the model predictions. The arrows indicate the behaviors of the brightness decline corresponding to various Δz , which is the difference in the magnitude of the two epochs for an interval of $\Delta t = 6$ days.

1st epoch for supernovae using the spectral template of Nugent et al. (2002). The points show Δz and $(i - z)_{1st}$ with a 1-day step from the day of the merger, and their time evolutions are connected by lines. The fastest decline observed for supernovae is approximately 0.5 mag in 6 days, and therefore, models of supernovae cannot explain the rapid decline of SSS17a. The wind model with medium Y_e ($Y_e = 0.25$) at $t = 1$ day or 2 days provides the best agreement with the observation.

The color evolution of SSS17a is also consistent with that of kilonova models. Figure 5 shows the $z - H$ and $J - H$ color curves of SSS17a as compared with those of the three kilonova models. The $J - H$ colors and the absence of the strong evolution are broadly consistent with the models. The $z - H$ color and its temporal reddening are similar to those of the models comprising Lanthanide elements. In contrast, the $z - H$ color of SSS17a is not consistent with the Lanthanide-free model (blue curve in Figure 5), i.e., the high opacities of Lanthanide elements provide a better description of SSS17a.

The properties of SSS17a, i.e., the rapid evolution, red color, and rapid reddening, are consistent with the standard model of a kilonova. The color evolution suggests that the ejecta contain a small amount of Lanthanide elements. This means that r -process nucleosynthesis beyond the 2nd peak takes place in the NS merger event GW170817/SSS17a. However, the absolute magnitude

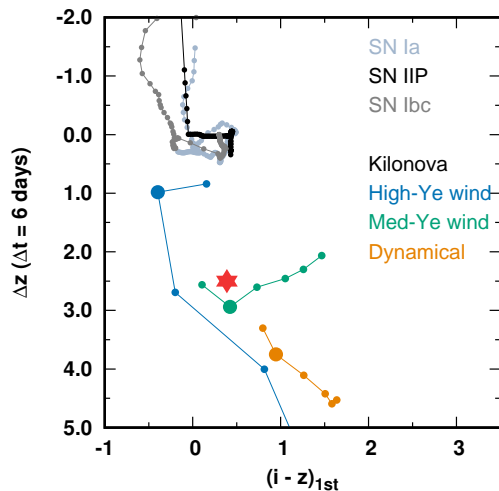


Fig. 4. The result of the photometry of SSS17a is plotted on Δz and $(i - z)_{1st}$ plane with kilonova and supernova models. For SSS17a (red symbol), Δz is the magnitude difference between the two epochs, $t = 1.7$ and 7.7 days ($\Delta t = 6$ days) after the detection of GW170817, and $(i - z)_{1st}$ is the color at the first epoch ($t = 1.7$ day). The models for kilonovae and supernovae are shown by colored dots and gray dots, respectively. Each dot corresponds to different starting epoch of Δt with an increment of 1 day. The larger dots in the kilonova model loci show the values for the case that the starting epoch of Δt is the 2nd day from the merger. The kilonova models are located far from the crowds of those for supernovae at 40 Mpc, especially in terms of Δz . The data point of SSS17a is consistent with the model of medium Y_e wind.

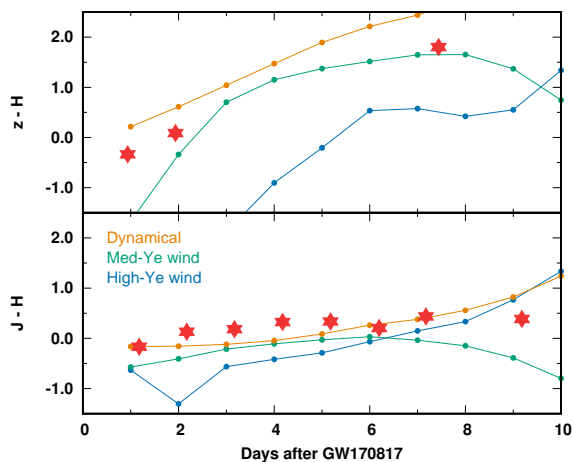


Fig. 5. Time evolution of $z - H$ and $J - H$ color compared with the kilonova models.

of the brightness of SSS17a is greater than that of the kilonova models of $M_{ej} = 0.01M_{\odot}$. This discrepancy can be explained by adopting a larger ejecta mass, e.g., $M_{ej} = 0.03M_{\odot}$, which gives a higher radioactive luminosity. Since the high ejecta mass makes the timescale of the longer, a higher ejecta velocity may also be required to keep the good agreement in the timescale shown in our

paper (Tanaka et al. in press). Or possibly, a higher luminosity can be accounted for by an additional energy source, such as the cocoon emission (Gottlieb et al. 2017).

5 Summary

We present J-GEM observations of SSS17a, a promising EM counterpart to GW170817. Intensive observations are performed with Subaru (z and K_s -band), IRSF (J , H , and K_s -band), B&C (g , r , and i -band), MOA-II (V and R -band), Nayuta (J , H , and K_s -band), Kanata (H -band), and MITSuME (g , r , and i -band) telescopes. SSS17a exhibits an extremely rapid decline in the z -band, which is not explained by any type of supernova at any epoch. In addition, the evolution of the color is quite rapid; the $z - H$ color is changed by approximately 2.5 mag in 7 days. We show that the observational properties, i.e., rapid evolution of the light curves, the red color, and its rapid evolution, are consistent with models of kilonovae having Lanthanide elements. This indicates that r -process nucleosynthesis beyond the second peak takes place in the NS merger event GW170817. However, the absolute magnitude of SSS17a is brighter than that of kilonova models of $M_{ej} = 0.01M_{\odot}$. This suggests that the mass ejection is more vigorous ($\sim 0.03M_{\odot}$) or that there is an additional energy source.

Acknowledgments

We are grateful to the staff of Subaru Telescope, South African Astronomical Observatory, and University of Canterbury Mt. John Observatory for their help for the observations of this work. We thank Dr. Masato Onodera and Prof. Takashi Nakamura who provided insightful comments, and Dr. Nobuhiro Okabe who provided a computational resource. This work was supported by MEXT KAKENHI (JP17H06363, JP15H00788, JP24103003, JP10147214, JP10147207) and JSPS KAKENHI (JP16H02183, JP15H02075, JP15H02069, JP26800103, JP25800103), the research grant program of the Toyota Foundation (D11-R-0830), the natural science grant of the Mitsubishi Foundation, the research grant of the Yamada Science Foundation, the National Institute of Natural Sciences (NINS) program for cross-disciplinary science study, Inoue Science Research Award from Inoue Foundation for Science, Optical & Near-Infrared Astronomy Inter-University Cooperation Program from the MEXT, and the National Research Foundation of South Africa. This work is based on data collected at the Subaru Telescope, which is operated by the National Astronomical Observatory of Japan, NINS.

References

- Abbott, B. P., et al. 2016a, Physical Review Letters, 116, 061102
- . 2016b, Physical Review Letters, 116, 241103
- . 2017, Physical Review Letters, 118, 221101

- Akitaya, H., et al. 2014, in Proc. SPIE, Vol. 9147, Ground-based and Airborne Instrumentation for Astronomy V, 91474O
- Barnes, J., & Kasen, D. 2013, *ApJ*, 775, 18
- Bertin, E. 2006, in Astronomical Society of the Pacific Conference Series, Vol. 351, Astronomical Data Analysis Software and Systems XV, ed. C. Gabriel, C. Arviset, D. Ponz, & S. Enrique, 112
- Bertin, E. 2011, in Astronomical Society of the Pacific Conference Series, Vol. 442, Astronomical Data Analysis Software and Systems XX, ed. I. N. Evans, A. Accomazzi, D. J. Mink, & A. H. Rots, 435
- Bertin, E., & Arnouts, S. 1996, *A&AS*, 117, 393
- Blanton, M. R., & Roweis, S. 2007, *AJ*, 133, 734
- Bosch, J., et al. 2017, ArXiv e-prints, arXiv:1705.06766
- Chambers, K. C., et al. 2016, ArXiv e-prints, arXiv:1612.05560
- Coulter, D. A., Kilpatrick, C. D., Siebert, M. R., Foley, R. J., J., S. B., Drout, M. R. Simon, J. S., & Piro, A. L. 2017, *GCN Circ.*, 21529
— in prep.
- Cutri, R. M., et al. 2003, *VizieR Online Data Catalog*, 2246
- Freedman, W. L., et al. 2001, *ApJ*, 553, 47
- Gottlieb, O., Nakar, E., & Piran, T. 2017, ArXiv e-prints, arXiv:1705.10797
- Kasen, D., Badnell, N. R., & Barnes, J. 2013, *ApJ*, 774, 25
- Kasen, D., Fernández, R., & Metzger, B. D. 2015, *MNRAS*, 450, 1777
- Koshimoto, N., et al. 2017, *AJ*, 154, 3
- Kotani, T., et al. 2005, *Nuovo Cimento C Geophysics Space Physics C*, 28, 755
- Kulkarni, S. R. 2005, arXiv:astro-ph/0510256, arXiv:astro-ph/0510256
- Lang, D., Hogg, D. W., Mierle, K., Blanton, M., & Roweis, S. 2010, *AJ*, 139, 1782
- Li, L.-X., & Paczyński, B. 1998, *ApJL*, 507, L59
- Metzger, B. D., & Fernández, R. 2014, *MNRAS*, 441, 3444
- Metzger, B. D., et al. 2010, *MNRAS*, 406, 2650
- Miyazaki, S., et al. 2012, in Proc. SPIE, Vol. 8446, Ground-based and Airborne Instrumentation for Astronomy IV, 84460Z
- Monet, D. G., et al. 2003, *AJ*, 125, 984
- Morokuma, T., et al. 2016, *PASJ*, 68, L9
- Nagayama, T., et al. 2003, in Proc. SPIE, Vol. 4841, Instrument Design and Performance for Optical/Infrared Ground-based Telescopes, ed. M. Iye & A. F. M. Moorwood, 459–464
- Nugent, P., Kim, A., & Perlmutter, S. 2002, *PASP*, 114, 803
- Peng, C. Y., Ho, L. C., Impey, C. D., & Rix, H.-W. 2002, *AJ*, 124, 266
- Sako, T., et al. 2008, *Experimental Astronomy*, 22, 51
- Sanders, N. E., et al. 2015, *ApJ*, 799, 208
- Schlafly, E. F., & Finkbeiner, D. P. 2011, *ApJ*, 737, 103
- Sumi, T., et al. 2016, *ApJ*, 825, 112
- Suzuki, R., et al. 2008, *PASJ*, 60, 1347
- Tanaka, M., & Hotokezaka, K. 2013, *ApJ*, 775, 113
- Tanaka, M., Hotokezaka, K., Kyutoku, K., Wanajo, S., Kiuchi, K., Sekiguchi, Y., & Shibata, M. 2014, *ApJ*, 780, 31
- Tanaka, M., et al. 2017, arXiv:1708.09101, arXiv:1708.09101
— in press
- The LIGO Scientific Collaboration and the Virgo Collaboration. 2017a, *GCN Circ.*, 21509
— 2017b, *GCN Circ.*, 21527
— 2017c, *GCN Circ.*, 21505
— in prep.
- Utsumi, Y., et al. in press
- Yoshida, M., et al. 2017, *PASJ*, 69, 9